Photon statistics

5

The task of quantum optics is to study the consequences of considering a beam of light as a stream of photons rather than as a classical wave. It turns out that the differences are rather subtle, and we have to look quite hard to see significant departures from the predictions of the classical theories. In this chapter we shall approach the subject from the perspective of the statistical properties of the photon stream. We shall study the three different types of photon statistics that can occur, namely: Poissonian, super-Poissonian, and sub-Poissonian. A key result that emerges is that the observation of Poissonian and super-Poissonian statistics in photodetection experiments is consistent with the classical theory of light, but not sub-Poissonian statistics. Hence the observation of sub-Poissonian photon statistics constitutes direct confirmation of the photon nature of light. Unfortunately, it transpires that sub-Poissonian light is very sensitive to optical losses and inefficient detection. This explains why it has only been observed relatively recently, following the development of high efficiency detectors.

The chapter concludes with a consideration of some of the practical consequences of the photon statistics. This will lead us to discuss the origin of shot noise in photodetectors, and to consider how it can be reduced by using light with sub-Poissonian statistics.

5.1 Introduction

We can introduce our discussion of photon statistics by considering the detection of a light beam by a photon counter as illustrated in Fig. 5.1. The photon counter consists of a very sensitive light detector such as a photomultiplier tube (PMT) or avalanche photodiode (APD) connected to an electronic counter. The detector produces short voltage pulses in response to the light beam and the counter registers the number of pulses that are emitted within a certain time interval set by the user. Photon counters thus operate in a very similar way to the Geiger counters used to count the particles emitted by the decay of radioactive nuclei.

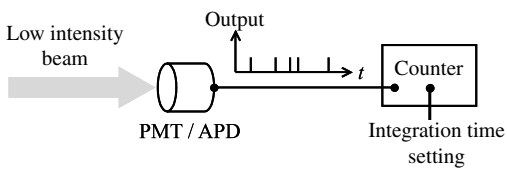

Fig. 5.1 Detection of a faint light beam by a PMT or APD and pulse counting electronics.

The analogy between a photon counter and a Geiger counter makes it apparent that the number of counts that we might expect to observe in a given time interval would not be constant. When using a Geiger counter, the count rate fluctuates about the average value due to the intrinsically random nature of the radioactive decay process. The same thing happens with a photon counter: the average count rate is determined by the intensity of the light beam, but the actual count rate fluctuates from measurement to measurement. It is these fluctuations in the count rate that are our concern here.

At first sight it might appear that the fact that the detector emits individual pulses is clear and conclusive evidence that the impinging light beam consists of a stream of discrete energy packets that we generally call 'photons'. The fluctuations in the count rate would then give information about the statistical properties of the incoming photon stream. Unfortunately, the argument is not quite that simple. It has been a long-standing issue in optical physics whether the individual events registered by photon counters are necessarily related to the photon statistics, or whether they are just an artefact of the detection process. This means that we have to distinguish carefully between:

(1) the statistical nature of the photodetection process;
(2) the intrinsic photon statistics of the light beam.

If we were approaching this subject from a historical perspective, it would make sense to look at the theory of photodetection first in order to avoid the danger of jumping to false conclusions. From a conceptual point of view, however, it is more interesting to examine the intrinsic statistical nature of the light first, and then return to consider how this relates to the results of photodetection experiments. It is this second approach that we adopt here.

In adopting an approach that starts from the photons, we are anticipating the final result that some experiments can *only* be explained if we attribute the photocount fluctuations to the underlying photon statistics. It must be emphasized, however, that the actual number of experiments that fall into this category is rather small. In Section 5.8.1 we shall show that *most* of the results obtained in photon-counting experiments can be explained by **semi-classical** models in which we treat the light classically but quantize the photoelectric effect in the detector. At the same time, this semi-classical approach tells us where to look for effects that *cannot* be explained by the classical theories of light. This second type of experiment is particularly interesting because it gives a clear proof of the quantum nature of light.

5.2 Photon-counting statistics

Let us consider the outcome of a photon-counting experiment as illustrated in Fig. 5.1. The basic function of the experiment is to count the

number of photons that strike the detector in a user-specified time interval T. We start with the simplest case and consider the detection of a perfectly coherent monochromatic beam of angular frequency ω and constant intensity I. In the quantum picture of light, we consider the beam to consist of a stream of photons. The **photon flux** Φ is defined as the average number of photons passing through a cross-section of the beam in unit time. Φ is easily calculated by dividing the energy flux by the energy of the individual photons:

$$\Phi = \frac{IA}{\hbar\omega} \equiv \frac{P}{\hbar\omega} \text{ photons s}^{-1}, \tag{5.1}$$

where A is the area of the beam and P is the power.

Photon-counting detectors are specified by their **quantum efficiency** η, which is defined as the ratio of the number of photocounts to the number of incident photons. The average number of counts registered by the detector in a counting time T is thus given by:

$$N(T) = \eta\Phi T = \frac{\eta PT}{\hbar\omega}. \tag{5.2}$$

The corresponding average **count rate** $\mathcal{R}$ is given by:

$$\mathcal{R} = \frac{N}{T} = \eta\Phi = \frac{\eta P}{\hbar\omega} \text{ counts s}^{-1}. \tag{5.3}$$

The maximum count rate that can be registered with a photon-counting system is usually determined by the fact that the detectors need a certain amount of time to recover after each detection event, which means that a 'dead time' of ~ 1 μs must typically elapse between successive counts. This sets a practical upper limit on $\mathcal{R}$ of around 10^6 counts s^{-1}. With typical values of η for modern detectors of 10% or more, eqn 5.3 shows that photon counters are only useful for analysing the properties of very faint light beams with optical powers of $\sim 10^{-12}$ W or less. The detection of light beams with higher power levels is done by a different method and will be discussed in Section 5.9.

The photon flux given in eqn 5.1 and the detector count rate given by eqn 5.3 both represent the *average* properties of the beam. A beam of light with a well-defined average photon flux will nevertheless show photon number fluctuations at short time intervals. This is a consequence of the inherent 'graininess' of the beam caused by chopping it up into photons. We can see this more clearly with the aid of a simple example.

Consider a beam of light of photon energy 2.0 eV with an average power of 1 nW. Such a beam could be obtained by taking a He:Ne laser operating at 633 nm with a power of 1 mW and attenuating it by a factor 10^6 by using appropriate filters. The average photon flux from eqn 5.1 is:

$$\Phi = \frac{10^{-9}}{2.0 \times (1.6 \times 10^{-19})} = 3.1 \times 10^9 \text{ photons s}^{-1}.$$

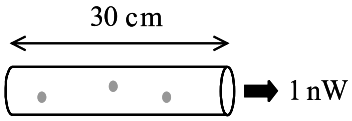

Fig. 5.2 A 30 cm section of a beam light at 633 nm with a power of 1 nW contains three photons on average.

Since the velocity of light is 3×10^8 m s^{-1}, a segment of the beam with a length of 3×10^8 m would contain 3.1×10^9 photons on average. On a smaller scale, we would expect an average of 31 photons within a 3 m segment of beam. In still smaller segments, the average photon number becomes fractional. For example, a 1-ns count time corresponds to a 30 cm segment of beam, and contains an average of 3.1 photons. Now photons are discrete energy packets, and the actual number of photons has to be an integer. We must therefore have an integer number of photons in each beam segment, as illustrated in Fig. 5.2. In the next section we shall show that if we assume that the photons are equally likely to be at any point within the beam, then we find random fluctuations above and below the mean value. If we were to look at 30 such beam segments, we might therefore find a sequence of photon counts that looks something like:

$$1, 6, 3, 1, 2, 2, 4, 4, 2, 3, 4, 3, 1, 3, 6, 5, 0, 4, 1, 1, 6, 2, 2, 6, 4, 1, 4, 3, 4, 6.$$

Statistical analysis of this sequence, which is based on uniform random numbers, gives a sum of 95, a mean of 3.16, and a standard deviation of 1.81. The statistical fluctuations arise from the fact that we do not know exactly where the photons are within the beam.

If we make the length of the segments even smaller, the fluctuations become even more apparent. For example, in a 3 cm segment of beam corresponding to a time interval of 100 ps, the average photon number falls to 0.31. The majority of beam segments are now empty, and a sequence of 10 beam segments equivalent to any one of the 30 cm segments considered above might look like:

1, 0, 0, 1, 0, 0, 0, 0, 0, 1.

This sequence has a sum of 3, a mean of 0.3, and a standard deviation of 0.46. It is apparent that the shorter the time interval, the more difficult it becomes to know where the photons are. Thus if we split the 30 cm beam segment shown in Fig. 5.2 into 1000 intervals of 0.3 mm length and 1 ps duration, we would find that typically only three intervals contain photons, and 997 are empty. We have no way of predicting which three of these 1000 segments contain the photons.

These examples show that although the average photon flux can have a well-defined value, the photon number on short time-scales fluctuates due to the discrete nature of the photons. These fluctuations are described by the **photon statistics** of the light. In the following sections, we shall investigate the statistical nature of various types of light, starting with the simplest case, namely a perfectly stable monochromatic light source.

5.3 Coherent light: Poissonian photon statistics

In classical physics, light is considered to be an electromagnetic wave. The most stable type of light that we can imagine is a perfectly coherent

light beam which has constant angular frequency ω, phase ϕ, and amplitude $\mathcal{E}_0$:

$$\mathcal{E}(x,t) = \mathcal{E}_0 \sin(kx - \omega t + \phi), \tag{5.4}$$

where $\mathcal{E}(x,t)$ is the electric field of the light wave and $k = \omega/c$ in free space. The beam emitted by an ideal single-mode laser operating well above threshold is a reasonably good approximation to such a field. The intensity I of the beam is proportional to the square of the amplitude (cf. eqn 2.28), and is constant if $\mathcal{E}_0$ and ϕ are independent of time. There will therefore be no intensity fluctuations and the average photon flux defined by eqn 5.1 will be constant in time.

The intensity is understood here to be determined by the average value of $\mathcal{E}(t)^2$ during an optical cycle.

It might be thought that a beam of light with a time-invariant average photon flux would consist of a stream of photons with regular time intervals between them. This is not in fact the case. We have seen above that there must be statistical fluctuations on short time-scales due to the discrete nature of the photons. We shall now show that perfectly coherent light with a constant intensity has **Poissonian** photon statistics.

Consider a light beam of constant power P. The average number of photons within a beam segment of length L is given by

$$\overline{n} = \Phi L/c, \tag{5.5}$$

where Φ is the photon flux given by eqn 5.1. We assume that L is large enough that $\overline{n}$ takes a well-defined integer value. We now subdivide the beam segment into N subsegments of length L/N. N is assumed to be sufficiently large that there is only a very small probability $p = \overline{n}/N$ of finding a photon within any particular subsegment, and a negligibly small probability of finding two or more photons.

We have assumed that p is the same for each subsegment because the intensity is identical at all points within the beam.

We now ask: what is the probability $\mathcal{P}(n)$ of finding n photons within a beam of length L containing N subsegments? The answer is given by the probability of finding n subsegments containing one photon and $(N-n)$ containing no photons, in any possible order. This probability is given by the binomial distribution:

$$\mathcal{P}(n) = \frac{N!}{n!(N-n)!}\, p^n\, (1-p)^{N-n}, \tag{5.6}$$

which, with $p = \overline{n}/N$, gives

$$\mathcal{P}(n) = \frac{N!}{n!(N-n)!}\, \left(\frac{\overline{n}}{N}\right)^n\, \left(1 - \frac{\overline{n}}{N}\right)^{N-n}. \tag{5.7}$$

We now take the limit as $N \to \infty$. To do this, we first rearrange eqn 5.7 in the following form:

$$\mathcal{P}(n) = \frac{1}{n!}\, \left(\frac{N!}{(N-n)!N^n}\right)\, \overline{n}^n\, \left(1 - \frac{\overline{n}}{N}\right)^{N-n}. \tag{5.8}$$

Now by using Stirling's formula:

$$\lim_{N\to\infty} [\ln N!] = N \ln N - N, \tag{5.9}$$

we can see that

$$\lim_{N\to\infty}\left[\ln\left(\frac{N!}{(N-n)!N^n}\right)\right]=0.$$

Hence:

$$\lim_{N\to\infty}\left[\frac{N!}{(N-n)!N^n}\right]=1. \tag{5.10}$$

Furthermore, by applying the binomial theorem and comparing the result for the limit $N\to\infty$ to the series expansion of $\exp(-\overline{n})$, we can see that:

$$\begin{aligned}\left(1-\frac{\overline{n}}{N}\right)^{N-n} &= 1-(N-n)\frac{\overline{n}}{N}+\frac{1}{2!}(N-n)(N-n-1)\left(\frac{\overline{n}}{N}\right)^2-\cdots\\ &\to 1-\overline{n}+\frac{\overline{n}^2}{2!}-\cdots\\ &= \exp(-\overline{n}).\end{aligned} \tag{5.11}$$

On using these two limits in eqn 5.8, we find

$$\lim_{N\to\infty}[\mathcal{P}(n)]=\frac{1}{n!}\cdot 1\cdot\overline{n}^n\cdot\exp(-\overline{n}). \tag{5.12}$$

We thus conclude that the photon statistics for a coherent light wave with constant intensity are given by:

$$\mathcal{P}(n)=\frac{\overline{n}^n}{n!}\mathrm{e}^{-\overline{n}},\quad n=0,\ 1,\ 2,\ \cdots. \tag{5.13}$$

This equation describes a **Poisson distribution**.

A summary of the mathematical properties of Poisson distributions may be found in Appendix A.

Poissonian statistics generally apply to random processes that can only return integer values. We have already mentioned one of the standard examples of Poissonian statistics, namely the number of counts from a Geiger tube pointing at a radioactive source. In this case, the number of counts is always an integer, and the average count value $\overline{n}$ is determined by the half life of the source, the amount of material present, and the time interval set by the user. The actual count values fluctuate above and below the mean value due to the random nature of the radioactive decay, and the probability for registering n counts is given by the Poissonian formula in eqn 5.13. A similar situation applies to the count rate of a photon-counting system detecting individual photons from a light beam with constant intensity. In this second case, the randomness originates from chopping the continuous beam into discrete energy packets with an equal probability of finding the energy packet within any given time subinterval.

Poisson distributions are uniquely characterized by their mean value $\overline{n}$. Representative distributions for $\overline{n}=0.1$, 1, 5, and 10 are shown in Fig. 5.3. It is apparent that the distribution peaks at $\overline{n}$ and gets broader as $\overline{n}$ increases. The fluctuations of a statistical distribution about its mean value are usually quantified in terms of the **variance**. The variance is equal to the square of the **standard deviation** Δn and is defined by:

$$\mathrm{Var}(n)\equiv(\Delta n)^2=\sum_{n=0}^{\infty}(n-\overline{n})^2\mathcal{P}(n). \tag{5.14}$$

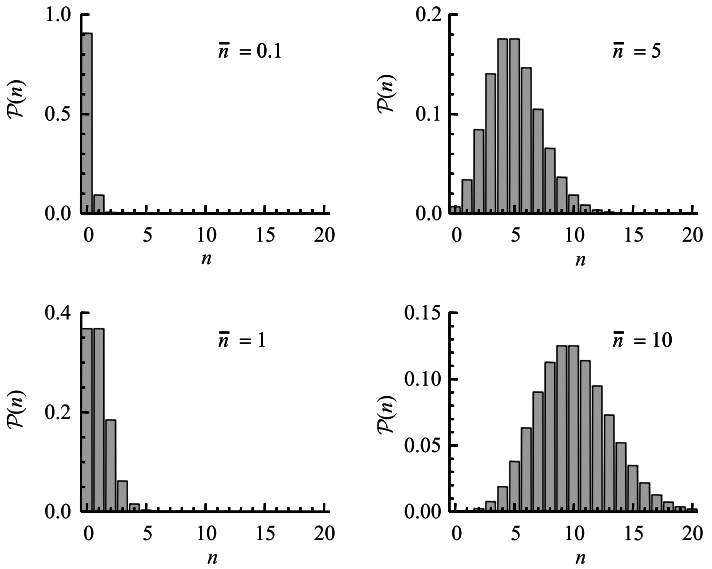

Fig. 5.3 Poisson distributions for mean values of 0.1, 1, 5, and 10. Note that the vertical axis scale changes between each figure.

It is a well-known result for Poisson statistics that the variance is equal to the mean value $\overline{n}$ (see eqn A.10):

$$(\Delta n)^2 = \overline{n}. \tag{5.15}$$

The standard deviation for the fluctuations of the photon number above and below the mean value is therefore given by:

$$\Delta n = \sqrt{\overline{n}}. \tag{5.16}$$

This shows that the relative size of the fluctuations decreases as $\overline{n}$ gets larger. If $\overline{n} = 1$, we have $\Delta n = 1$ so that $\Delta n/\overline{n} = 1$. On the other hand, if $\overline{n} = 100$, we have $\Delta n = 10$, and $\Delta n/\overline{n} = 0.1$.

Example 5.1 An attenuated beam from an argon laser operating at 514 nm (2.41 eV) with a power of 0.1 pW is detected with a photon-counting system of quantum efficiency 20% with the time interval set at 0.1 s. Calculate (a) the mean count value, and (b) the standard deviation in the count number.

Solution

(a) We first calculate the photon flux from eqn 5.1. This gives

$$\Phi = \frac{10^{-13}\ \text{W}}{2.41\ \text{eV}} = 2.59 \times 10^5\ \text{photon s}^{-1}.$$

The average photon count is then given by eqn 5.2:

$$N = 0.2 \times (2.59 \times 10^5) \times 0.1 = 5180.$$

(b) We assume that the detected counts have Poissonian statistics with a standard deviation given by eqn 5.16. With $\overline{n} \equiv N = 5180$, we then find:

$$\Delta n = \sqrt{5180} = 72.$$

5.4 Classification of light by photon statistics

In the previous section, we considered the photon statistics of a perfectly coherent light beam with constant optical power P. We saw that the statistics are described by a Poisson distribution with photon number fluctuations that satisfy eqn 5.16. From a classical perspective, a perfectly coherent beam of constant intensity is the most stable type of light that can be envisaged. This therefore provides a bench mark for classifying other types of light according to the standard deviation of their photon number distributions. In general, there are three possibilities:

- **sub-Poissonian statistics**: $\Delta n < \sqrt{\overline{n}}$,
- **Poissonian statistics**: $\Delta n = \sqrt{\overline{n}}$,
- **super-Poissonian statistics**: $\Delta n > \sqrt{\overline{n}}$.

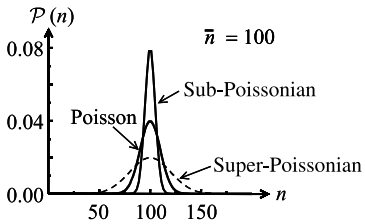

Fig. 5.4 Comparison of the photon statistics for light with a Poisson distribution, and those for sub-Poissonian and super-Poissonian light. The distributions have been drawn with the same mean photon number $\overline{n} = 100$. The discrete nature of the distributions is not apparent in this figure due to the large value of $\overline{n}$.

The difference between the three different types of statistics is illustrated in Fig. 5.4. This figure compares the photon number distributions of super-Poissonian and sub-Poissonian light to that of a Poisson distribution with the same mean photon number. We see that distributions of super-Poissonian and sub-Poissonian light are, respectively, broader or narrower than the Poisson distribution.

It is not difficult to think of types of light which would be expected to have super-Poissonian statistics. If there are any classical fluctuations in the intensity, then we would expect to observe larger photon number fluctuations than for the case with a constant intensity. Since a perfectly stable intensity gives Poissonian statistics, it follows that all classical light beams with time-varying light intensities will have super-Poissonian photon number distributions. In the next section we shall see that the thermal light from a black-body source and the partially coherent light from a discharge lamp fall into this category. These types of light are clearly 'noisier' than perfectly coherent light in both the classical sense that they have larger variations in the intensity, and also in the quantum sense that they have larger photon number fluctuations.

Sub-Poissonian light, by contrast, has a narrower distribution than the Poissonian case and is therefore 'quieter' than perfectly coherent light. Now we have already emphasized that a perfectly coherent beam is the most stable form of light that can be envisaged in classical optics. It is therefore apparent that sub-Poissonian light has no classical counterpart, and is therefore the first example of **non-classical light** that we have met. Needless to say, the observation of sub-Poissonian light is quite difficult, which explains why it is not normally discussed in standard optics texts.

Table 5.1 gives a summary of the classification of light according to the criteria established in this section.

Table 5.1 Classification of light according to the photon statistics. $I(t)$ is the time dependence of the optical intensity.

Photon statistics	Classical equivalents	$I(t)$	Δn
Super-Poissonian	Partially coherent (chaotic), incoherent, or thermal light	Time-varying	$> \sqrt{\overline{n}}$
Poissonian	Perfectly coherent light	Constant	$\sqrt{\overline{n}}$
Sub-Poissonian	None (non-classical)	Constant	$< \sqrt{\overline{n}}$

5.5 Super-Poissonian light

In this section we shall consider two examples of super-Poissonian statistics, namely thermal light and chaotic light. We have seen above that super-Poissonian light is defined by the relation:

$$\Delta n > \sqrt{\overline{n}}. \tag{5.17}$$

In the next chapter we shall see that super-Poissonian statistics can be related to **photon bunching**. In this present chapter, we concentrate on the statistical classification of the sources as determined by a photon-counting experiment.

We have also mentioned that super-Poissonian photon statistics have a classical interpretation in terms of fluctuations in the light intensity. It is always easier to make an unstable light source than a stable one, and therefore the observation of super-Poissonian statistics is commonplace. At the same time, it is important to understand the properties of super-Poissonian sources since they are frequently used in the laboratory.

5.5.1 Thermal light

The electromagnetic radiation emitted by a hot body is generally called **thermal light** or **black-body radiation**. The properties of thermal light are conventionally understood by applying the laws of statistical mechanics to the radiation within an enclosed cavity at a temperature T. The radiation pattern consists of a continuous spectrum of oscillating modes, with the energy density within the angular frequency range ω to $\omega + \mathrm{d}\omega$ given by Planck's law:

$$\rho(\omega, T)\ \mathrm{d}\omega = \frac{\hbar\omega^3}{\pi^2 c^3}\ \frac{1}{\exp(\hbar\omega/k_\mathrm{B}T) - 1}\ \mathrm{d}\omega. \tag{5.18}$$

The derivation of eqn 5.18 requires that the energy of the radiation should be quantized. We can consider each individual mode as a harmonic oscillator of angular frequency ω, and write down the quantized energy as (cf. eqn 3.93):

$$E_n = (n + \tfrac{1}{2})\hbar\omega, \tag{5.19}$$

In quantum optics, we interpret eqn 5.19 as meaning that there are n photons excited at angular frequency ω in the particular mode.

where n is an integer ≥ 0.

We consider a single radiation mode within the cavity at angular frequency ω. The probability that there will be n photons in the mode is given by Boltzmann's law:

$$\mathcal{P}_\omega(n) = \frac{\exp(-E_n/k_\mathrm{B}T)}{\sum_{n=0}^{\infty}\exp(-E_n/k_\mathrm{B}T)}. \tag{5.20}$$

The subscript on $\mathcal{P}(n)$ makes it plain that the probability refers specifically to a single mode at angular frequency ω.

On substituting E_n from eqn 5.19, we find:

$$\mathcal{P}_\omega(n) = \frac{\exp(-n\hbar\omega/k_\mathrm{B}T)}{\sum_{n=0}^{\infty}\exp(-n\hbar\omega/k_\mathrm{B}T)}, \tag{5.21}$$

which is of the form:

$$\mathcal{P}_\omega(n) = \frac{x^n}{\sum_{n=0}^{\infty}x^n}, \tag{5.22}$$

where

$$x = \exp(-\hbar\omega/k_\mathrm{B}T). \tag{5.23}$$

The general result for the summation of a geometric progression is:

$$\sum_{i=1}^{k} r^{i-1} \equiv \sum_{j=0}^{k-1} r^j = \frac{1-r^k}{1-r}, \tag{5.24}$$

which implies:

$$\sum_{n=0}^{\infty} x^n = \frac{1}{1-x}, \tag{5.25}$$

since $x < 1$. We therefore find:

$$\begin{aligned}\mathcal{P}_\omega(n) &= x^n(1-x)\\ &\equiv \Big(1-\exp(-\hbar\omega/k_\mathrm{B}T)\Big)\ \exp(-n\hbar\omega/k_\mathrm{B}T).\end{aligned} \tag{5.26}$$

The mean photon number is given by:

$$\begin{aligned}\overline{n} &= \sum_{n=0}^{\infty} n\ \mathcal{P}_\omega(n)\\ &= \sum_{n=0}^{\infty} nx^n(1-x)\\ &= (1-x)x\ \frac{\mathrm{d}}{\mathrm{d}x}\left(\sum_{n=0}^{\infty}x^n\right)\\ &= (1-x)x\ \frac{\mathrm{d}}{\mathrm{d}x}\left(\frac{1}{1-x}\right)\\ &= (1-x)x\ \frac{1}{(1-x)^2}\\ &= \frac{x}{(1-x)},\end{aligned} \tag{5.27}$$

which, on substitution from eqn 5.23, gives the Planck formula:

$$\overline{n} = \frac{1}{\exp(\hbar\omega/k_\mathrm{B}T)-1}. \tag{5.28}$$

Equation 5.27 implies that $x = \overline{n}/(\overline{n}+1)$, and we are thus able to rewrite the probability given in eqn 5.26 in terms of $\overline{n}$ as:

$$\mathcal{P}_\omega(n) = \frac{1}{\overline{n}+1}\left(\frac{\overline{n}}{\overline{n}+1}\right)^n. \tag{5.29}$$

This distribution is called the **Bose–Einstein distribution**. From eqn 5.26 we can see that $\mathcal{P}_\omega(n)$ is always largest for $n = 0$, and decreases exponentially for increasing n.

Figure 5.5 compares the photon statistics for a single mode of thermal light with the Bose–Einstein distribution to those of a Poisson distribution with the same value of $\overline{n}$. It is apparent that the distribution of photon numbers for thermal light is much broader than for Poissonian light. This is hardly surprising, given the nature of thermal energy fluctuations. The variance of the Bose–Einstein distribution can be found by inserting $\mathcal{P}_\omega(n)$ from eqn 5.29 into eqn 5.14, giving (see Exercise 5.3):

$$(\Delta n)^2 = \overline{n} + \overline{n}^2. \tag{5.30}$$

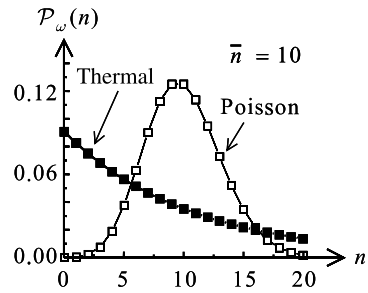

Fig. 5.5 Comparison of the photon statistics for a single mode of a thermal source and a Poisson distribution with the same value of $\overline{n} = 10$.

This shows that the variance of the Bose–Einstein distribution is always larger than that of a Poisson distribution (cf. eqn 5.15), and that thermal light therefore falls into the category of super-Poissonian light defined by eqn 5.17. For example, if $\overline{n} = 10$ as in Fig. 5.5, we have $\Delta n = 3.2$ for the Poisson distribution, but $\Delta n = 10.5$ for thermal light.

It should be stressed that the Bose–Einstein distribution only applies to a *single mode* of the radiation field. In reality, black-body radiation consists of a continuum of modes, and in most experiments we have to consider the properties of multi-mode thermal light. It can be shown that the photon number variance of N_m thermal modes of similar frequency is given by:

$$(\Delta n)^2 = \overline{n} + \frac{\overline{n}^2}{N_\mathrm{m}}, \tag{5.31}$$

which reduces to the result for a Poisson distribution when N_m is large. In practice, it is very difficult to measure a single mode of the thermal field, and the statistics measured in most experiments with thermal light will therefore be Poissonian. (See Exercise 5.5.)

The derivation of eqn 5.31 may be found, for example, in Mandel and Wolf (1995, §13.3.2). It should also be pointed out that if the detection time interval is long, the intensity fluctuations will be averaged out, and Poisson counting statistics will be obtained even for single-mode thermal light. This point will be explained further in the next subsection.

The single-mode variance given in eqn 5.30 can be interpreted in an interesting way if we refer to Einstein's analysis of the energy fluctuations of back-body radiation originally given in 1909. According to statistical mechanics, the magnitude of the energy fluctuations from the mean value at thermal equilibrium $\langle E\rangle$ is given by:

$$\langle \Delta E^2\rangle = k_\mathrm{B}T^2\,\frac{\partial\langle E\rangle}{\partial T}. \tag{5.32}$$

See Pais (1982, §21a).

If we apply this result to the energy fluctuations of black-body radiation in the angular frequency range ω to $\omega + \mathrm{d}\omega$, we obtain:

$$\begin{aligned}\langle \Delta E^2 \rangle \, \mathrm{d}\omega &= k_\mathrm{B} T^2 \, \frac{\partial}{\partial T}(V \rho \, \mathrm{d}\omega) \\ &= k_\mathrm{B} T^2 V \, \mathrm{d}\omega \, \frac{\partial \rho}{\partial T} \\ &= \left(\rho \hbar\omega + \frac{\pi^2 c^3}{\omega^2} \rho^2 \right) V \, \mathrm{d}\omega, \end{aligned} \tag{5.33}$$

where V is the volume of the cavity, and ρ is the spectral energy density given by the Planck formula (eqn 5.18). These energy fluctuations can be connected to the photon number fluctuations per mode by writing:

$$\begin{aligned}\langle \Delta E^2 \rangle \, \mathrm{d}\omega &= \text{density of states} \times \text{energy fluctuations per mode} \times \text{volume} \\ &= \frac{\omega^2}{\pi^2 c^3} \, \mathrm{d}\omega \times \left\langle \left(\Delta(n\hbar\omega) \right)^2 \right\rangle \times V \\ &= \frac{\omega^2}{\pi^2 c^3} \, (\Delta n)^2 \, (\hbar\omega)^2 \, V \, \mathrm{d}\omega, \end{aligned} \tag{5.34}$$

where we made use of eqn C.11 in Appendix C for the density of states. On comparing eqns 5.33 and 5.34 we find that:

$$(\Delta n)^2 = \frac{\pi^2 c^3}{\hbar\omega^3} \rho + \left(\frac{\pi^2 c^3}{\hbar\omega^3} \rho \right)^2 . \tag{5.35}$$

Then, by using eqn 5.28 to rewrite eqn 5.18 as:

$$\rho = \frac{\hbar\omega^3}{\pi^2 c^3} \, \overline{n}, \tag{5.36}$$

we find as before (cf. eqn 5.30):

$$(\Delta n)^2 = \overline{n} + \overline{n}^2. \tag{5.37}$$

The same argument applies to the first and second terms in eqn 5.37: the first term which gives the Poissonian statistics arises from the quantization of the light, while the second is caused by classical intensity fluctuations.

Einstein realized that the first term in eqn 5.33 originates from the particle nature of the light, while the second originates from the thermal fluctuations of the energy of the electromagnetic radiation. The latter term is therefore classical in origin, and is called the **wave noise**. The first term, by contrast, originates from the quantization of the energy of the electromagnetic radiation, that is, the photon nature of light.

5.5.2 Chaotic (partially coherent) light

Note that the use of the term 'chaotic' for partially coherent light predates chaos theory. Chaos theory has nothing to do with chaotic light.

The light from a single spectral line of a discharge lamp is generally called **chaotic light**. Chaotic light has partial coherence, with classical intensity fluctuations on a time-scale determined by the coherence time τ_c. (See Section 2.3.) These intensity fluctuations will obviously give rise to greater fluctuations in the photon number than for a source with a constant power (i.e. a perfectly coherent source).

It can be shown that the fluctuations in the photocount rate when a chaotic source is incident on a detector are given by:

See, for example, Mandel and Wolf (1995, §9.7), or Goodman (1985, §9.2).

$$(\Delta n)^2 = \langle W(T) \rangle + \langle \Delta W(T)^2 \rangle, \tag{5.38}$$

where W represents the count rate in the detection time interval T:

$$W(T) = \int_t^{t+T} \eta \Phi(t') \, \mathrm{d}t', \tag{5.39}$$

η being the detection efficiency and $\Phi(t)$ the instantaneous photon flux given by eqn 5.1. The mean count rate $\langle W(t) \rangle$ is of course equal to $\overline{n}$. If there were no intensity fluctuations so that $\Phi(t)$ was constant, then eqn 5.38 would just revert to the Poissonian case with $(\Delta n)^2 = \overline{n}$.

In chaotic light, the photon flux is *not* constant due to the fluctuations in the intensity of the light on time-scales of the order of the coherence time. These intensity fluctuations will be significant if the measurement time T is comparable to, or less than, the coherence time τ_c. The second term in eqn 5.38 would then be non-zero, implying that chaotic light, when measured on short time-scales, is super-Poissonian. On the other hand, when $T \gg \tau_\mathrm{c}$, the intensity fluctuations on time-scales of order τ_c will not be noticed, and the intensity may be taken as effectively constant. In this case we again revert to the Poissonian formula.

See Loudon (2000, §3.9), especially eqns 3.9.22 and 3.9.23.

The two terms in eqn 5.38 can be interpreted as originating, respectively, from the Poissonian statistics associated with the particle nature of light and the classical power fluctuations in the source. The classical fluctuations due to the time-varying intensity of the source are often called wave noise in analogy with the case of black-body radiation considered in the previous subsection.

5.6 Sub-Poissonian light

Sub-Poissonian light is defined by the relation:

$$\Delta n < \sqrt{\overline{n}}. \tag{5.40}$$

It is apparent from Fig. 5.4 that sub-Poissonian light has a narrower photon number distribution than for Poissonian statistics. We have seen in Section 5.3 that a perfectly coherent beam with constant intensity has Poissonian photon statistics. We thus conclude that sub-Poissonian light is somehow more stable than perfectly coherent light, which has been our paradigm up to this point. In fact, sub-Poissonian light has no classical equivalent. Therefore, the observation of sub-Poissonian statistics is a clear signature of the quantum nature of light.

In the next chapter, we shall see that sub-Poissonian photon statistics are often associated with the observation of another purely quantum optical effect, namely photon **antibunching**.

Even though there is no direct classical counterpart of sub-Poissonian light, it is easy to conceive of conditions that would give rise to sub-Poissonian statistics. Let us consider the properties of a beam of light in which the time intervals Δt between the photons are identical, as

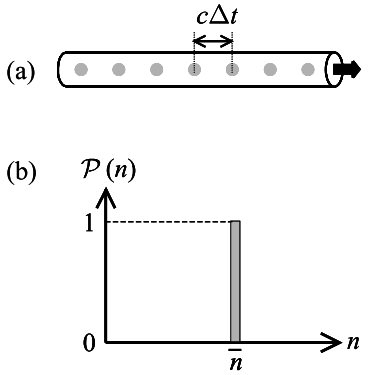

Fig. 5.6 (a) A beam of light containing a stream of photons with a fixed time spacing Δt between them. (b) Photon-counting statistics for such a beam.

illustrated schematically in Fig. 5.6(a). The photocount obtained for such a beam in a time T would be the integer value determined by:

$$N = \text{Int}\left(\eta \frac{T}{\Delta t}\right), \tag{5.41}$$

which would be exactly the same for every measurement. The experimenter would therefore obtain the histogram shown in Fig. 5.6(b), with $\overline{n} = N$ given by eqn 5.41. This is highly sub-Poissonian, and has $\Delta n = 0$.

Photon streams of the type shown in Fig. 5.6(a) with $\Delta n = 0$ are called **photon number states**. Further details of photon number states will be given in Chapter 8. Photon number states are the purest form of sub-Poissonian light. Other types of sub-Poissonian light can be conceived in which the time intervals between the photons in the beam are not exactly the same, but are still more regular than the random time intervals appropriate to a beam with Poissonian statistics. Such types of light are fairly easy to generate in the laboratory, although their detection is quite problematic, and will be discussed in Section 5.10.

5.7 Degradation of photon statistics by losses

It should be apparent from the discussion in the previous section that light with sub-Poissonian statistics is particularly interesting. In Section 5.10 we shall discuss how such light might be observed in the laboratory. Before we do this, we need to cover an important issue related to optical losses.

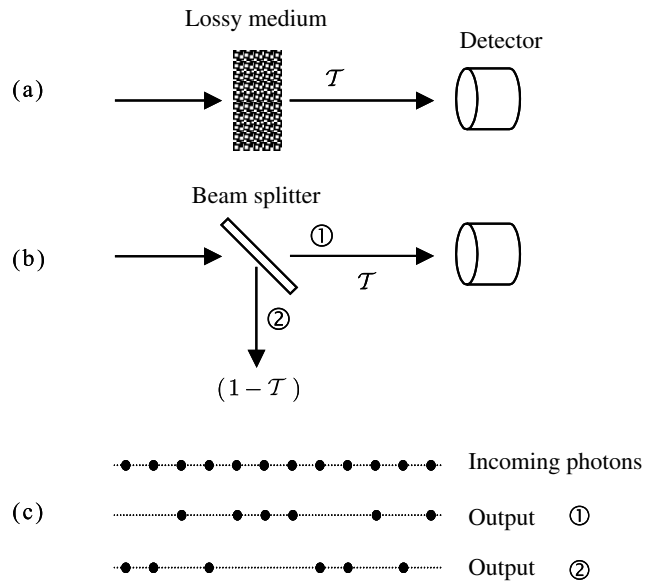

Fig. 5.7 (a) The effect of a lossy medium with transmission $\mathcal{T}$ on a beam of light can be modelled as a beam splitter with splitting ratio $\mathcal{T} : (1 - \mathcal{T})$ as shown in (b). The beam splitting process is probabilistic at the level of the individual photons, and so the incoming photon stream splits randomly towards the two outputs with a probability set by the transmission : reflection ratio (50 : 50 in this case) as shown in part (c).

Let us suppose that we have a beam of light that passes through a lossy medium and is then detected as shown in Fig. 5.7(a). If the transmission of the medium is $\mathcal{T}$, then we can model the losses as a beam splitter with splitting ratio $\mathcal{T} : (1 - \mathcal{T})$, as indicated in Fig. 5.7(b). The beam splitter separates the photons into two streams going towards its two output ports, so that only a fraction $\mathcal{T}$ of the incoming photons impinge on the detector and are registered as counts. Now the beam splitting process occurs randomly at the level of individual photons, with weighted probabilities for the two output paths of $\mathcal{T} : (1 - \mathcal{T})$, respectively. We therefore see that the lossy medium randomly selects photons from the incoming beam with probability $\mathcal{T}$. It is well known that the distribution obtained by **random sampling** of a given set of data is more random than the original distribution. This point is illustrated in Fig 5.7(c), which presents the case of a regular stream of photons split with $50 : 50$ probability towards two output ports. It is apparent that the regularity of the time intervals in the photon stream going to the detector is reduced compared to the incoming photon stream. Thus the random sampling nature of optical losses degrades the regularity of the photon flux, and would eventually make the time intervals completely random for low values of $\mathcal{T}$.

The beam splitter model of optical losses is a convenient way to consider the many different factors that reduce the efficiency of photon-counting experiments. These factors include:

(1) inefficient collection optics, whereby only a fraction of the light emitted from the source is collected;

(2) losses in the optical components due to absorption, scattering, or reflections from the surfaces;

(3) inefficiency in the detection process due to using detectors with imperfect quantum efficiency.

All of these processes are equivalent to random sampling of the photons. The first one randomly selects photons from the source. The second randomly deletes photons from the beam. The third randomly selects a subset of photons to be detected. The first two degrade the photon statistics themselves, while the third degrades the correlation between the photon statistics and the photoelectron statistics.

This argument unfortunately shows that sub-Poissonian light is very fragile: all forms of loss and inefficiency will tend to degrade the statistics to the Poissonian (random) case. This means that we must be very careful to avoid optical losses and use very high-efficiency detectors to observe large quantum effects in the photon statistics.

5.8 Theory of photodetection

The relationship between the photon and detection statistics has been a contentious issue in quantum optics, and has only been definitively resolved in relatively recent times.

Now that we are familiar with the different types of photon statistics that can occur, it is appropriate to consider the relationship between the counting statistics registered by the detector and the underlying

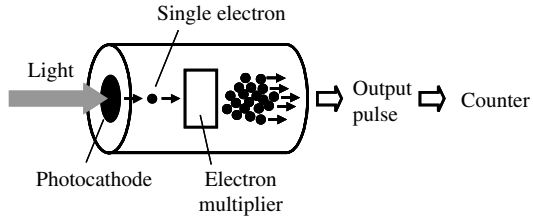

Fig. 5.8 Schematic diagram of the operation of a single-photon counting photomultiplier. The incident light ejects single electrons from the photocathode, which then trigger the release of an avalanche of electrons in the multiplier region, thereby generating an output pulse large enough to be detected by electronics.

photon statistics of the light beam. We start by outlining the semi-classical theory of photodetection in which the light is assumed to consist of classical electromagnetic waves. This will enable us to highlight the critical results that prove that the light beam really does consist of a stream of photons. We shall then give the results for the full quantum theory of photodetection, and hence see the conditions under which non-classical effects can be observed.

5.8.1 Semi-classical theory of photodetection

Single-photon avalanche photodiode (SPAD) detectors are now also commonly used for single-photon counting experiments.

Let us consider a photon-counting detector such as a photomultiplier illuminated by a faint light beam, as shown in Fig. 5.8. The light interacts with the atoms in the photocathode of the detector and liberates individual electrons by the photoelectric effect. These single photoelectrons then trigger the release of many more electrons in the multiplier region of the tube, thereby generating a current pulse of sufficient magnitude to be detected with an electronic counter. The pulses counted thus correspond to the release of individual electrons from the photocathode.

In the following we assume that the light beam is a classical electromagnetic wave of intensity I. The atoms in the photocathode are assumed to be quantized so that the photoelectrons are ejected in a probabilistic fashion after the absorption of a quantum of energy from the light beam. The statistical nature of the timing between the output pulses can then be explained by the making the following three assumptions about the photodetection process:

See, for example, Goodman (1985).

1. The probability of the emission of a photoelectron in a short time interval Δt is proportional to the intensity I, the area A illuminated, and the time interval Δt.
2. If Δt is sufficiently small, the probability of emitting two photoelectrons is negligibly small.
3. Photoemission events registered in different time intervals are statistically independent of each other.

From assumption (1) we can write the probability of observing one photoemission event in the time interval $t \to t + \Delta t$ as:

$$\mathcal{P}(1; t, t + \Delta t) = \xi I(t) \Delta t, \tag{5.42}$$

where ξ is proportional to the area illuminated and is equal to the emission probability per unit time per unit intensity. Assumption (2) then

implies that the probability of observing no events in the same time interval is given by:

$$\mathcal{P}(0;t,t+\Delta t) = 1 - \mathcal{P}(1;t,t+\Delta t) = 1 - \xi I(t)\Delta t. \tag{5.43}$$

We now ask: what is the probability of obtaining n events in the time interval $0 \to t+\Delta t$? If the events are statistically independent (assumption 3) and Δt is small, then there are only two ways of achieving this result: n events in the time interval $0 \to t$ and none in time interval $t \to t+\Delta t$, or $n-1$ events in time interval $0 \to t$ and one in time interval $t \to t+\Delta t$. We must therefore have:

$$\begin{aligned}\mathcal{P}(n;0,t+\Delta t) &= \mathcal{P}(n;0,t)\mathcal{P}(0;t,t+\Delta t) + \mathcal{P}(n-1;0,t)\mathcal{P}(1;t,t+\Delta t) \\ &= \mathcal{P}(n;0,t)[1-\xi I(t)\Delta t] + \mathcal{P}(n-1;0,t)\xi I(t)\Delta t. \end{aligned} \tag{5.44}$$

On writing $\mathcal{P}(n;0,t) \equiv \mathcal{P}_n(t)$ and rearranging, we find:

$$\frac{\mathcal{P}_n(t+\Delta t) - \mathcal{P}_n(t)}{\Delta t} = \xi I(t)[\mathcal{P}_{n-1}(t) - \mathcal{P}_n(t)], \tag{5.45}$$

which, on taking the limit $\Delta t \to 0$, gives:

$$\frac{\mathrm{d}\mathcal{P}_n(t)}{\mathrm{d}t} = \xi I(t)\left[\mathcal{P}_{n-1}(t) - \mathcal{P}_n(t)\right]. \tag{5.46}$$

The general solution to this recursion relation, with the boundary condition $\mathcal{P}_0(0) = 1$, is:

$$\mathcal{P}_n(t) = \frac{\left[\int_0^t \xi I(t')\,\mathrm{d}t'\right]^n}{n!} \exp\left(-\int_0^t \xi I(t')\;\mathrm{d}t'\right). \tag{5.47}$$

The derivation of eqn 5.47 is beyond the scope of this book. We can, however, show that the solution is correct for the simplest case in which $I(t)$ is constant, that is independent of t. With $\xi I = \text{constant} \equiv C$, eqn 5.46 reduces to:

Constant intensity corresponds to perfectly coherent light.

$$\frac{\mathrm{d}\mathcal{P}_n(t)}{\mathrm{d}t} + C\mathcal{P}_n(t) = C\mathcal{P}_{n-1}(t). \tag{5.48}$$

For $n = 0$ it must be the case that $\mathcal{P}_{n-1}(t) = 0$ because we cannot have a negative count value. The first recursion relation is therefore of the form:

$$\frac{\mathrm{d}\mathcal{P}_0(t)}{\mathrm{d}t} = -C\mathcal{P}_0(t), \tag{5.49}$$

which, with the boundary condition $\mathcal{P}_0(0) = 1$, has the solution:

$$\mathcal{P}_0(t) = \exp(-Ct). \tag{5.50}$$

For $n \geq 1$ we multiply eqn 5.48 by the integrating factor e^{Ct} to obtain:

$$\frac{\mathrm{d}}{\mathrm{d}t}\left(\mathrm{e}^{Ct}\mathcal{P}_n(t)\right) = C\mathrm{e}^{Ct}\mathcal{P}_{n-1}(t), \tag{5.51}$$

which, on integrating, gives:

$$\mathcal{P}_n(t) = \mathrm{e}^{-Ct} \int_0^t C\mathrm{e}^{Ct'} \mathcal{P}_{n-1}(t')\ \mathrm{d}t'. \tag{5.52}$$

With $\mathcal{P}_0(t)$ given by eqn 5.50, we can then solve recursively to obtain:

$$\begin{aligned}
\mathcal{P}_1(t) &= \mathrm{e}^{-Ct} \int_0^t C\mathrm{e}^{Ct'} \mathcal{P}_0(t')\ \mathrm{d}t' = (Ct)\ \mathrm{e}^{-Ct}, \\
\mathcal{P}_2(t) &= \mathrm{e}^{-Ct} \int_0^t C\mathrm{e}^{Ct'} \mathcal{P}_1(t')\ \mathrm{d}t' = \frac{(Ct)^2}{2}\ \mathrm{e}^{-Ct}, \\
\mathcal{P}_3(t) &= \mathrm{e}^{-Ct} \int_0^t C\mathrm{e}^{Ct'} \mathcal{P}_2(t')\ \mathrm{d}t' = \frac{(Ct)^3}{3!}\ \mathrm{e}^{-Ct}, \\
&\vdots \\
\mathcal{P}_n(t) &= \mathrm{e}^{-Ct} \int_0^t C\mathrm{e}^{Ct'} \mathcal{P}_{n-1}(t')\ \mathrm{d}t' = \frac{(Ct)^n}{n!}\ \mathrm{e}^{-Ct}.
\end{aligned} \tag{5.53}$$

Since $\int_0^t \xi I(t')\mathrm{d}t' = \xi It = Ct$ if $I(t)$ is constant, it is evident that eqn 5.53 is consistent with eqn 5.47.

We can cast eqn 5.53 into a more familiar form if we notice that eqn 5.42 implies that the event probability per unit time is equal to $\xi I(t)$. Therefore, if $I(t)$ is constant, the mean count rate $\overline{n}$ for the time interval $0 \rightarrow t$ is just given by:

$$\overline{n} = \xi It \equiv Ct. \tag{5.54}$$

Hence we can rewrite eqn 5.53 as

$$\mathcal{P}_n(t) = \frac{\overline{n}^n}{n!}\mathrm{e}^{-\overline{n}}, \tag{5.55}$$

which shows that we obtain a Poisson distribution when $I(t)$ is constant. (cf. eqn 5.13.)

Equation 5.55 demonstrates that we can explain the Poissonian photocount statistics observed when detecting light with a time-independent intensity without invoking the concept of photons at all. All that we require is that the emission of photoelectrons is a probabilistic process triggered by the absorption of a quantum of energy from the light beam. Hence the analysis of the photocount statistics does not necessarily tell us anything about the underlying photon statistics. At the same time, it is clear that sub-Poissonian statistics are not possible within a semi-classical theory. This follows because we obtain the Poissonian formula if the intensity is constant, and if the intensity varies with time, it can be shown that we obtain the super-Poissonian result given in eqn 5.38. Hence the observation of *sub*-Poissonian photocount statistics constitutes a clear demonstration that the semi-classical approach is inadequate. In Section 5.10 we shall describe experimental work that gives direct evidence of sub-Poissonian photodetection statistics. These experiments can *only* be explained by the full quantum treatment of light detection, and definitively establish the quantum nature of light.

5.8.2 Quantum theory of photodetection

The aim of the quantum theory of photodetection is to relate the photocount statistics observed in a particular experiment to those of the incoming photons. The derivation of the final result is beyond the scope of this work, and at this level we can only quote the conclusion and discuss its implications at a qualitative level.

Students who wish to pursue the quantum theory of photodetection in more detail are referred to the more advanced texts. See, for example, Mandel and Wolf (1995, Chapter 14), or Loudon (2000, §6.10).

As usual, we consider the photocount statistics measured in a time interval of T. We are interested in the relationship between the variance in the photocount number $(\Delta N)^2$ and the corresponding variance $(\Delta n)^2$ in the number of photons impinging on the detector in the same time interval. This relationship is given by:

$$(\Delta N)^2 = \eta^2(\Delta n)^2 + \eta(1-\eta)\overline{n}, \tag{5.56}$$

See, for example, Loudon (2000, eqn 6.10.8).

where η is the quantum efficiency of the detector, defined previously as the ratio of the average photocount number $\overline{N}$ to the mean photon number $\overline{n}$ incident on the detector in the same time interval (cf. eqn 5.2):

$$\eta = \frac{\overline{N}}{\overline{n}}. \tag{5.57}$$

Several important conclusions follow from eqn 5.56.

1. If $\eta = 1$, we have $\Delta N = \Delta n$ and the photocount fluctuations faithfully reproduce the fluctuations of the incident photon stream.
2. If the incident light has Poissonian statistics with $(\Delta n)^2 = \overline{n}$, then $(\Delta N)^2 = \eta\overline{n} \equiv \overline{N}$ for all values of η. In other words, the photocount statistics always give a Poisson distribution.
3. If $\eta \ll 1$, the photocount fluctuations tend to the Poissonian result with $(\Delta N)^2 = \eta\overline{n} \equiv \overline{N}$ irrespective of the underlying photon statistics.

The conclusion is obvious: if we want to measure the photon statistics we need high efficiency detectors. If we have such detectors, the photocount statistics give a true measure of the incoming photon statistics, with a fidelity that increases as the efficiency of the detector increases.

It is apparent from the comments above that the quantum efficiency of the detector is the critical parameter that determines the relationship between the photoelectron and photon statistics. We can understand why this should be so by reference to Fig. 5.7(b). An imperfect detector of efficiency η is equivalent to a perfect detector of 100% efficiency with a beam splitter of transmission η in front of it. As discussed in Section 5.7, the random sampling nature of the beam-splitting process gradually randomizes the statistics, irrespective of the original statistics of the incoming photons. In the limit of very low efficiencies, the time intervals between the photoelectrons would become completely random, and the counting statistics would be Poissonian for all possible incoming distributions.

The difficulty in producing single-photon detectors with high quantum efficiencies is one of the reasons why it is difficult to observe sub-Poissonian statistics in the laboratory. With low efficiency detectors,

the photocount statistics will always be random (i.e. Poissonian), irrespective of the incoming photon distribution. Nowadays, however, single-photon detectors with quantum efficiencies in excess of 50% are available for some wavelengths. Furthermore, by using a different detection strategy employing high-intensity beams and photodiode detection, quantum efficiencies approaching 90% can be obtained. This is the topic of the next section.

5.9 Shot noise in photodiodes

Photodiodes, in contrast to the detectors used for single-photon counting (i.e. photomultipliers or *avalanche* photodiodes), do not contain electron multiplication regions. Hence there is a one-to-one relationship between the number of photoelectrons generated in the active region of the photodiode and the number of photons incident on the detector. This should not be misinterpreted to imply that it is the *same* electron that was excited to the conduction band by the photon that flows in the external circuit: the correspondence between individual electrons and photons is lost by the myriad of electron–electron scattering processes that occur in the semiconductor material and in the wires. However, the charge flow is conserved throughout the circuit, and it is this that determines the current that is measured by the detection electronics.

Up to this point, we have been thinking exclusively about the detection of light beams by single-photon counting methods as sketched in Fig. 5.1. As mentioned in Section 5.2, this method is only appropriate for very weak beams with a flux of $\sim 10^6$ photons s^{-1} or less. In many cases we shall be dealing with light beams of much higher photon flux. For example, a He:Ne laser beam with a power of 1 mW at 633 nm has, from eqn 5.1, a flux of 3.3×10^{15} photons s^{-1}. No detector can respond fast enough to register the individual photons in this case, and we would completely saturate the output of a single-photon counting detector such as a photomultiplier. A different detection strategy must therefore be used.

The normal method used to detect high flux light beams is to employ **photodiode** detectors. Photodiodes are semiconductor devices that generate electrons in an external circuit when photons excite electrons from the valence band to the conduction band. A key parameter of a photodiode is its quantum efficiency η, which is defined in this context as the ratio of the number of photoelectrons generated in the external circuit to the number of photons incident. Hence the current generated in the external circuit for an incident photon flux Φ, namely the **photocurrent** i, is given by:

$$i = \eta e \Phi \equiv \eta e \frac{P}{\hbar\omega}, \tag{5.58}$$

where e is the modulus of the charge of the electron, P is the power of the beam, and ω is its angular frequency (cf. eqn 5.1). The ratio $i/P = \eta e/\hbar\omega$ is called the **responsivity** of the photodiode and has the units of $\mathrm{A\,W}^{-1}$. The value of η can therefore be worked out from the measured responsivity at the detection wavelength.

Well-designed photodiodes can have quantum efficiencies in excess of 90%.

Figure 5.9(a) gives a schematic representation of the detection of a high-intensity light beam with a photodiode (PD) detector. The light is incident on the detector, and the time dependence of the resulting photocurrent is displayed on an oscilloscope after appropriate amplification. Alternatively, the photocurrent is analysed in the frequency domain by using a spectrum analyser. Figure 5.9(b) gives a simplified circuit diagram for the detection system. The photocurrent $i(t)$ flows through a load resistor R_L, thereby generating a time-dependent voltage $i(t)R_\mathrm{L}$. The capacitor C blocks the DC component of the voltage, and the AC part is then amplified to produce the output voltage $V(t)$. Measurement

A spectrum analyser is an electronic device that displays the Fourier transform of the time-dependent voltage at its input.

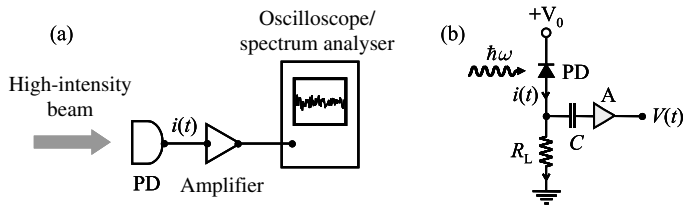

Fig. 5.9 (a) Detection of a high-intensity light beam with a photodiode (PD) detector. The time dependence of the photocurrent fluctuations relates to the photon statistics of the incoming beam. (b) Simplified diagram for the detector circuit. The diode is reverse-biased with a voltage V_0. The photocurrent $i(t)$ generated in the detector flows through a load resistor $R_{\rm L}$, and the AC voltage across $R_{\rm L}$ is amplified to produce a time-dependent output voltage $V(t)$. The capacitor C blocks the DC voltage across $R_{\rm L}$ from saturating the amplifier A.

of the DC voltage across $R_{\rm L}$ permits the average photocurrent $\langle i \rangle$ to be determined.

The principle behind using photodiode detectors to study the statistical properties of light is that the photocurrent generated by the beam will fluctuate because of the underlying fluctuations in the impinging photon number. These photon number fluctuations will be reflected in the photocurrent fluctuations with a fidelity determined by η. The fluctuations manifest themselves as **noise** in the photocurrent, as illustrated in Fig 5.10(a). The time-varying photocurrent $i(t)$ can be broken into a time-independent average current $\langle i \rangle$ and a time-varying fluctuation $\Delta i(t)$ according to:

$$i(t) = \langle i \rangle + \Delta i(t). \tag{5.59}$$

The average value of $\Delta i(t)$ must, of course, be zero, but the average of the square of Δi, namely $\langle (\Delta i(t))^2 \rangle$, will not be zero. Since the photocurrent flows through the load resistor $R_{\rm L}$, which then generates energy at the rate of $i^2 R_{\rm L}$, it is convenient to analyse the fluctuations in terms of a time-varying **noise power** according to:

$$P_{\rm noise}(t) = (\Delta i(t))^2 R_{\rm L}. \tag{5.60}$$

The Fourier transform of this noise power can be displayed on a spectrum analyser after suitable amplification. Figure 5.10(b) shows the type of noise power spectrum that might typically be obtained.

Let us consider what happens if we illuminate the photodiode with the light from a single-mode laser operating high above threshold. Such light is nearly perfectly coherent, and is expected to have Poissonian photon statistics, in which the photon number fluctuations obey eqn 5.15. The photoelectron statistics will therefore also follow a Poisson distribution with:

$$(\Delta N)^2 = \langle N \rangle. \tag{5.61}$$

Since $i(t)$ is proportional to the number of photoelectrons generated per second, it follows that the photocurrent variance Δi will satisfy:

$$(\Delta i)^2 \propto \langle i \rangle. \tag{5.62}$$

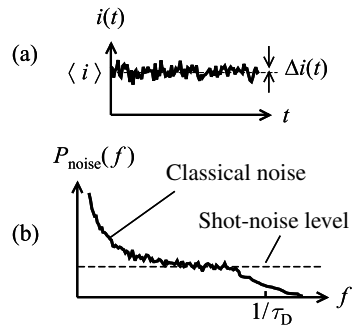

Fig. 5.10 (a) Time-varying photocurrent resulting from the detection of a high-intensity light beam with a photodiode detector as in Fig. 5.9. $\langle i \rangle$ represent the average photocurrent, while Δi represents the fluctuation from the mean value. (b) Fourier transform of $(\Delta i(t))^2$ showing the typical dependence of the photocurrent noise on frequency f. It is assumed that the photodiode used to detect the light has a response time of $\tau_{\rm D}$, and that the light source has excess classical noise at low frequencies.

The term 'shot noise' was originally used to describe the random spread of the pellets from a shot gun. Electrical shot noise was extensively studied in the days of vacuum tube electronics. The current in a vacuum tube is ultimately determined by the random thermal emission of electrons from the hot cathode, and thus exhibits Poissonian statistics. Simple ohmic circuits with a battery and a resistor, by contrast, do not usually exhibit shot noise. Instead, they have Johnson noise, which arises from the thermal fluctuations of the current.

On taking the Fourier transform of $i(t)$ and then measuring the variance of the current fluctuations within a frequency bandwidth Δf, we find:

$$(\Delta i)^2 = 2e\Delta f \ \langle i \rangle. \tag{5.63}$$

The corresponding noise power is given from eqn 5.60 as:

$$P_{\text{noise}}(f) = 2eR_{\text{L}}\Delta f \ \langle i \rangle. \tag{5.64}$$

The fluctuations described by eqns 5.63 and 5.64 are called **shot noise**.

Two characteristic features of shot noise are apparent from eqns 5.63 and 5.64:

- The variance of the current fluctuations (or equivalently, the noise power) is directly proportional to the average value of the current.
- The noise spectrum is 'white', that is, independent of frequency.

The second characteristic is a consequence of the random timing between the arrival of the photons in a beam with Poissonian statistics. The 'whiteness' of the noise, is, of course, subject to the response time τ_{D} of the photodiode, which means that in practice the shot noise can only be detected up to a maximum frequency of $\sim (1/\tau_{\text{D}})$. This point is illustrated in the schematic representation of the noise power spectrum shown in Fig. 5.10(b).

All light sources will show some classical intensity fluctuations due to noise in the electrical drive current, and lasers are subject to additional classical noise due to mechanical vibrations in the cavity mirrors. These classical noise sources tend to produce intensity fluctuations at fairly low frequencies, and so the noise spectrum tends to be well above the shot noise level in the low-frequency limit. However, at high frequencies, the classical noise sources are no longer present, and we are left with only the fundamental noise caused by the photon statistics. Hence a typical spectrum will show a noise level well above the shot noise limit at low frequencies, but should eventually reach the shot noise limit at high frequencies as shown in Fig. 5.10(b). Shot noise is present at all frequencies and the high frequency roll-off shown in Fig. 5.10(b) only reflects the frequency limit imposed by the detector response time.

In the semi-classical theory of photodetection, the shot noise level corresponding to Poissonian photoelectron statistics is the fundamental detection limit. Hence the shot noise power level is often called the **quantum limit** or **standard quantum limit** of detection. For a similar reason, shot noise is often called **quantum noise**.

Figure 5.11 shows the noise spectrum measured for a Nd:YAG laser operating at 1064 nm. The noise power is specified in 'dBm' units, which is a logarithmic scale defined by:

The decibel scale itself gives a logarithmic representation of a ratio r as $10 \times \log_{10} r$.

$$\text{Power in dBm units} = 10 \times \log_{10}\left(\frac{\text{Power}}{1 \text{ mW}}\right). \tag{5.65}$$

The data clearly show that the laser exhibits classical noise at low frequencies, but ultimately reaches the shot-noise limit at around 15 MHz.

The linear relationship between the shot noise and the photocurrent predicted by eqn. 5.64 is demonstrated by the data plotted in Fig. 5.12. This shows the high-frequency photocurrent noise power of a Ti:sapphire laser as a function of the optical power incident on the detector. The data show a linear increase in the noise power with the optical power.

Since the average photocurrent is directly proportional to the average power via eqn 5.58, the results clearly demonstrate the linear relationship between the shot noise and the average current.

The low-frequency classical noise that is apparent in Fig. 5.11 can, in principle, be removed. Two ways in which this might be done are shown in Fig. 5.13, namely the '**noise eater**' and the **balanced detector**. Consider first the noise eater shown in Fig. 5.13(a). The figure shows an intensity stabilization scheme in which a signal proportional to the laser output is fed back to the power supply. Negative feedback is used, so that the output of the power supply is reduced to compensate for fluctuations of the laser power above the average value, and vice versa. Alternatively, a modulator could be placed after the laser with a negative input proportional to the laser output, so that high-intensity fluctuations get attenuated more. These schemes can compensate (to a greater or lesser extent) for the classical power fluctuations in the laser output, but can do nothing about the shot noise, which is intrinsic to the light and cannot be removed by any classical stabilization methods. The best that such a stabilization scheme can hope to achieve is to remove all the excess classical noise and bring the output noise level down to the shot-noise level.

Now consider the balanced detector scheme shown in Fig. 5.13(b). The output of the laser is split into two beams of equal intensity, which are then detected with two identical photodiodes D1 and D2, generating photocurrents i_1 and i_2, respectively. The outputs of the photodiodes are connected so that the subtracted signal $(i_1 - i_2)$ can be detected. From a classical perspective, the two currents should be identical, so that the output signal is zero. If an absorbing sample S is introduced into the path leading to D2, i_2 will decrease and a positive signal will result. In this way, it is possible to measure very small absorption levels from, say, thin film samples. Alternatively, it is possible to detect a very weak modulation signal applied to one of the beams after the beam splitter.

The key point about the balanced detector scheme is that it usually gives much better signal-to-noise ratios than a single detector. If only a single detector were to be used, the small change in the intensity caused by the presence of the sample might be lost in the laser noise. With balanced detectors, by contrast, the classical noise is exactly cancelled (at least in principle) by the subtraction of the photocurrents, and much smaller changes in the intensity should be resolvable. Note, however, that the balanced detection scheme *cannot* remove the shot noise. From the perspective of the photons, the 50 : 50 beam splitting process is random, and therefore any noise associated with the photon nature of the light cannot be cancelled. Since the quantum nature of the light gives rise to shot noise, the output of the balanced detectors with no sample present will correspond to the shot-noise level.

It should by now be clear that shot noise is very important in optical science and telecommunications because it sets a practical limit to the signal-to-noise ratios that can be obtained in normal circumstances. For example, we can encode information onto a laser beam by modulating its intensity at a particular frequency. The information is retrieved by analysing the time-dependence of the photocurrent generated in the

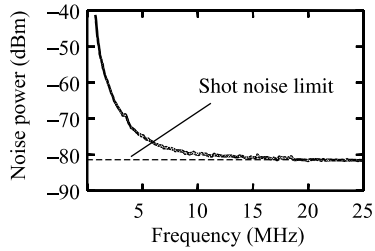

Fig. 5.11 Laser intensity noise spectrum measured for a Nd:YAG laser operating at 1064 nm with a fast detector of reponsivity 0.7 A W^{-1}. The detection bandwidth was 100 kHz, and the optical power and average photocurrent were 66 mW and 46 mA, respectively. (After D.J. Ottaway *et al.*, *Appl. Phys. B* **71**, 163 (2000), reproduced with permission of Springer Science and Business Media.)

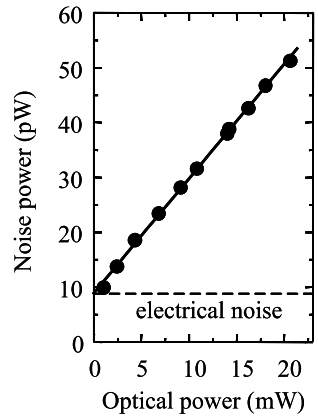

Fig. 5.12 Power dependence of the amplified photocurrent noise at 50 MHz within a 3 MHz bandwidth measured for a Ti:sapphire laser operating at 930 nm. The offset at zero power is caused by the ever-present electrical noise in the detector circuit. This noise is uncorrelated with the photocurrent noise, and so the two noise sources just add together, leading to the constant offset observed in the data. (Data by the author.)

We shall come across balanced detectors again in Section 7.8. In that discussion, we shall analyse the balanced detector from a different perspective and assign the shot noise output with no sample present to the vacuum modes that enter the unused input port of the 50 : 50 beam splitter.

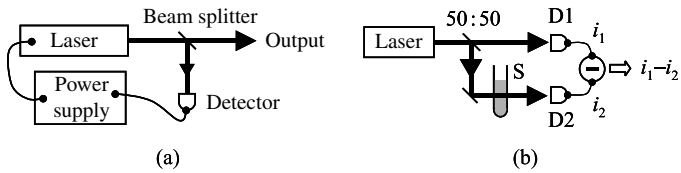

Fig. 5.13 (a) Noise eater scheme for stabilizing the power output of a laser. The laser power is monitored by sending a portion of the output to a detector from a beam-splitter. The detected signal is then used to control the power supply to the laser in a negative feedback loop. (b) Balanced detection scheme for cancelling classical noise. The beam is split into two equal parts by a 50 : 50 beam splitter, which are then incident on identical detectors D1 and D2. The output is equal to the difference of the photocurrents i_1 and i_2 from D1 and D2. When a sample S is inserted into the path to D2, the intensities on the detectors are no longer balanced, which then gives rise to a positive output.

receiving circuit. The size of the detected photocurrent signal must be larger than the photocurrent fluctuations due to the laser noise, and a glance at Fig. 5.11 suggests that the best strategy is to work at high frequencies where the laser noise is smallest. At these frequencies the laser noise is determined by the photon statistics set by the shot-noise limit. Hence the shot noise imposes a basic limit on the minimum signal-to-noise ratio that can be achieved. The only way to beat the shot noise limit is to use non-classical light sources with sub-Poissonian photon statistics. (See Section 5.10 below.)

The presence of shot noise in the photocurrent generated by the detection of light raises similar questions about its origin as arise with the observation of Poissonian statistics in a photon-counting detector. In analogy to the discussion of eqn 5.56 for photon-counting statistics, the photoelectron statistics from a photodiode will always show a Poisson distribution if the detector is inefficient. Moreover, we would also expect to observe shot noise after the detection of a purely classical light wave of constant intensity due to the probabilistic nature of the photodetection process at the microscopic level. In the next section we shall see that noise levels below the shot limit have been obtained in a number of experiments using sub-Poissonian light and high-efficiency detectors. This is not understandable within the semi-classical approach in which the noise originates in the photodetection process, and establishes that the shot noise in a high-efficiency photodiode can originate from the light, not the detector.

Example 5.2 A 10 mW He:Ne laser operating at 632.8 nm is detected with a photodiode of responsivity of 0.43 $\mathrm{A\,W^{-1}}$ via a load resistor of 50 Ω. Calculate:

(a) the quantum efficiency of the detector,

(b) the average photocurrent,

(c) the root-mean-square (r.m.s.) current fluctuations within a bandwidth of 100 kHz,

(d) the noise power measured in dBm units after amplification by an amplifier with a power gain of 20 dB in the same 100 kHz bandwidth.

Solution

(a) The quantum efficiency is worked out from the responsivity via eqn 5.58:

$$\eta = \frac{\hbar\omega}{e} \times \frac{i}{P} = 1.96 \text{ V} \times 0.43 \text{ A W}^{-1} = 84\%.$$

(b) The photocurrent is worked out from the responsivity:

$$i(\text{A}) = \text{responsivity } (\text{A W})^{-1} \times \text{power (W)} = 0.43 \times 0.01 = 4.3 \text{ mA}.$$

(c) The variance of the current fluctuations within the bandwidth Δf is given by eqn 5.63. Hence the r.m.s. fluctuation for the photocurrent worked out above is given by:

$$\Delta i_{\text{r.m.s.}} = \sqrt{2e\Delta f \ \langle i \rangle} = (2e \times 10^5 \times 0.0043)^{1/2} = 12 \text{ nA}.$$

(d) The noise power in the load resistor is given by eqn 5.64 as:

$$P_{\text{noise}} = 2e \times 50 \times 10^5 \times 0.0043 = 6.9 \times 10^{-15} \text{ W}.$$

An amplification factor of +20 dB implies a power gain of $10^{(+20/10)} = 100$. Hence the amplified shot noise power would be 6.9×10^{-13} W, which, from eqn 5.65, is equivalent to −91.6 dBm.

5.10 Observation of sub-Poissonian photon statistics

The demonstration of sub-Poissonian photon statistics depends on two key aspects:

- the discovery of light sources with sub-Poissonian statistics;
- the development of detectors with high quantum efficiencies.

In practice, the second point has been a severe limitation, because, as eqn 5.56 demonstrates, there is no hope of demonstrating sub-Poissonian photoelectron statistics with a detector of low quantum efficiency. Fortunately, high-efficiency detectors are now readily available for many wavelengths. This has led to an increasing number of demonstrations of sub-Poissonian light. In the following two subsections we concentrate on the methods for the direct generation of sub-Poissonian light from light sources driven by electrical power supplies.

Other methods to generate sub-Poissonian light will be covered in Chapters 6–7. Sections 6.6 and 6.7 describe the generation of antibunched light, while Section 7.9.2 describes the generation of amplitude squeezed light by nonlinear optics. Note, however, that antibunched light is not necessarily sub-Poissonian: see the discussion in Section 6.5.3.

5.10.1 Sub-Poissonian counting statistics

Figure 5.14 shows an experimental scheme for generating sub-Poissonian light at 253.7 nm. The experiment works on the principle that the time taken by the atoms to emit a photon is short compared to the time-scales of the fluctuations in the electrical current used to excite the atoms.

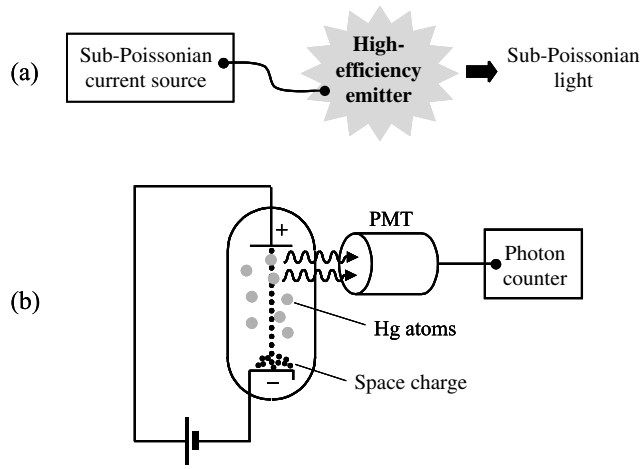

Fig. 5.14 (a) General scheme for generating sub-Poissonian light by driving a high-efficiency light emitter with a current source with sub-Poissonian electron statistics. (b) Experimental scheme for generating sub-Poissonian ultraviolet light at 253.7 nm from Hg atoms in a Franck–Hertz tube. The tube was operated in the space-charge-limited mode in which the electron statistics were sub-Poissonian. The photons were detected with a photomultiplier (PMT) and a photon counter. (After M.C. Teich and B. E. A. Saleh, *J. Opt. Soc. Am. B* **2**, 275 (1985).)

This implies that the statistical properties of the photons emitted in a discharge tube are closely related to the statistical properties of the electrons that comprise the current. It is intuitively obvious that if the electron flow is completely regular, then the photon flux is also regular, with equal time spacing between the photons. This point is summarized schematically in Fig. 5.14(a). Such a stream of photons is highly sub-Poissonian and contrasts with the usual (Poissonian) case in which the time spacing is random. The efficiency of the emission process needs to be high for the method to work well. If it is not, only a random subset of the electrons generate photons, and, as discussed in Section 5.7, such random sampling eventually randomizes the statistics, whatever the properties of the original photon distribution.

The experimental arrangement used to generate the sub-Poissonian light is illustrated schematically in Fig. 5.14(b). The light source consists of a Franck–Hertz tube filled with mercury (Hg) atoms. These atoms emit photons at 4.887 eV (253.7 nm) after excitation by electrons with sufficient energy to generate the photon. The electrons that comprise the anode current in the discharge tube are generated by thermal emission from the cathode and their energy is determined by the voltage between the anode and cathode. The statistics of the electrons generated by thermal emission would normally be random (i.e. Poissonian). However, it is well known that at the relatively small tube voltages required to initiate the mercury emission (i.e. 4.887 V), a space charge develops around the cathode. The presence of the space charge tends to regularize the electron flow, so that the statistics of the electrons in the anode current

are sub-Poissonian. The photons emitted when the electrons collide with the mercury atoms are thus expected to have sub-Poissonian statistics.

The light measured in the experiment shown in Fig. 5.14 was found to have a variance smaller than the Poissonian value by 0.16%. The reason why the measured effect was so small was that the overall efficiency for conversion of electrons in the anode current to photoelectrons in the PMT was only 0.25%. This low efficiency was caused by a product of factors, including: the inefficiency of the electron–atom excitation process (25%), the imperfect photon collection efficiency (10%), the imperfect transmission of the optics (83%), and the imperfect quantum efficiency of the detector (15%). Although the light generated was only very slightly sub-Poissonian, the experiment was a clear proof of principle and paved the way for the experiments described in the next subsection which produce much larger effects.

It is instructive to consider briefly why it is so much easier to generate a sub-Poissonian current in an electrical circuit than it is to generate sub-Poissonian light. It is obvious that the negatively charged electrons repel each other. Furthermore, electrons are fermions and it is not possible for two of them to occupy the same quantum state. Both of these effects tend to keep the electrons apart, and hence to produce regular streams, randomized only by relatively small thermal fluctuations. Neither of these two regularizing mechanisms works for photons, which are neutral bosons, and can bunch together or spread themselves randomly with ease.

5.10.2 Sub-shot-noise photocurrent

The principle for generating sub-Poissonian light shown in Fig. 5.14(a) can readily be extended to solid-state emitters such as light-emitting diodes (LEDs) or laser diodes (LDs), which have much higher efficiencies than discharge tubes. Figure 5.15(a) shows a scheme for generating sub-Poissonian light from an LED and detecting it with a photodiode

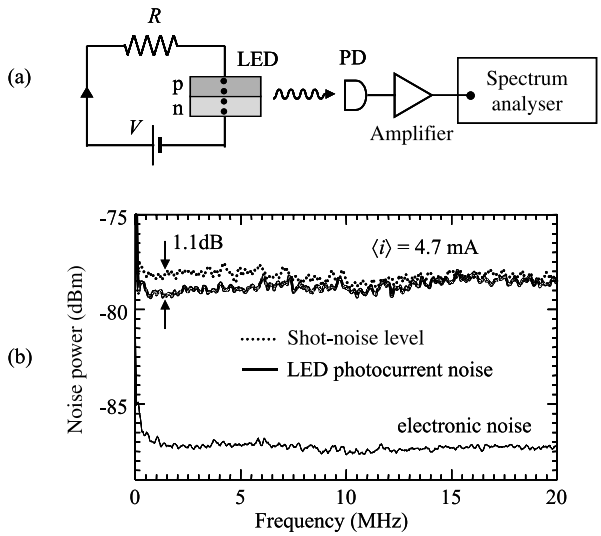

Fig. 5.15 (a) Generation of sub-Poissonian light from a high-efficiency LED and detection with a photodiode (PD). (b) Amplified photocurrent noise power spectrum measured for an AlGaAs LED emitting at 875 nm and measured with a photodiode of quantum efficiency 90%. The average photocurrent detected was 4.7 mA, and the detection bandwidth was 30 kHz. The curve shown by the dotted line corresponds to the calibrated shot-noise limit for the same current of 4.7 mA. The amplifier noise was about 9 dB below the shot-noise level, as shown by the lower curve in the graph. (After F. Wölfl *et al.*, *J. Mod. Opt.* **45**, 1147 (1998). © Taylor and Francis, reproduced with permission.)

detector. In this case the LED is driven by a battery with a series resistor R in the drive circuit. The purpose of the resistor is to control the current that flows, and in these circumstances the current fluctuations are determined by the thermal (Johnson) noise in the resistor. Provided the voltage dropped across the resistor is greater than $2k_{\mathrm{B}}T/e$, where T is the temperature, then the fluctuations in the drive current are below the shot noise level. (See Exercise 5.12.) With $2k_{\mathrm{B}}T/e \sim 50$ mV at room temperature, this condition is easily achieved, and the drive current is then strongly sub-Poissonian. If the LED has high efficiency, then the photon statistics should reflect the sub-Poissonian character of the drive current.

Figure 5.15(b) show typical results obtained for a commercial AlGaAs LED operating at 875 nm. The photocurrent noise is observed to lie approximately 1.1 dB (21%) below the shot-noise level at frequencies of around 1 MHz. At higher frequencies the photocurrent noise tends to the shot-noise level due to the inability of the LED to follow the drive current at frequencies above its modulation response limit (~ 5 MHz). The observation of photocurrent noise below the shot-noise level clearly indicates that the photon statistics emitted by the LED are sub-Poissonian.

The experiments to demonstrate sub-shot-noise photocurrents have to be calibrated very carefully when the optical power level on the detector is high. This is because the photodiode response tends to saturate at high powers, and this can lead to erroneous measurements of the photocurrent noise.

It is convenient to quantify the shot-noise reduction in terms of the **Fano factor** F_{Fano} defined by:

$$F_{\mathrm{Fano}} = \frac{\text{measured noise}}{\text{shot noise limit}}. \tag{5.66}$$

The Fano factor for the data shown in Fig. 5.15(b) is thus 0.79 at ~ 1 MHz. If the total efficiency of the system in converting drive electrons from the battery into photoelectrons in the detector circuit is η_{total}, then the measured Fano factor is expected to be:

See H.A. Bachor *et al.*., *Appl. Phys. B* **55**, 258 (1992).

$$F_{\mathrm{Fano}} = \eta_{\mathrm{total}} F_{\mathrm{dr}} + (1 - \eta_{\mathrm{total}}), \tag{5.67}$$

where F_{dr} is the noise level of the drive current relative to the shot noise level. With $F_{\mathrm{dr}} = 1$, we find $F_{\mathrm{Fano}} = 1$ for all values of η_{total}, but for a strongly sub-Poissonian drive current, we have $F_{\mathrm{dr}} \to 0$ and $F_{\mathrm{Fano}} \to (1 - \eta_{\mathrm{total}})$. The Fano factor of 0.79 deduced from the data in Fig. 5.15(b) agreed closely with the total conversion efficiency deduced from the product of the LED emission efficiency, the photon collection efficiency, and the detector quantum efficiency.

The principle shown in Fig. 5.15 is also applicable to semiconductor laser diodes. The use of such lasers in optical experiments has been shown to result in signal-to-noise ratios substantially better than the shot-noise level. Laser diodes offer a number of advantages over LEDs in the context of sub-shot-noise light generation. They usually have higher emission efficiencies and also emit into preferred directions, making the photon collection more efficient. Furthermore, they have large gain bandwidths, leading to the generation of sub-shot-noise light up to very high frequencies. The down-side is that laser diodes are far more sensitive to other noise sources than LEDs. In

particular, they are very sensitive to instabilities in the power distribution between the longitudinal modes of the cavity. This means that most laser diodes show noise levels well above the shot-noise limit at all frequencies. In practice, the generation of sub-shot-noise light from laser diodes usually requires single-mode lasers with very high modal purities, often incorporating mode stabilization techniques employing external cavities.

Further reading

More advanced treatments of photon statistics may be found, for example, in Mandel and Wolf (1995) or Loudon (2000). Both texts give a thorough treatment of the semi-classical and quantum theories of photoelectric detection, while the semi-classical approach is also well described in Goodman (1985). Bachor and Ralph (2004) give a detailed explanation of the experimental techniques required to measure sub-Poissonian light, while Yamamoto and Imamoglu (1999) describe the theory of sub-Poissonian light generation by LEDs and laser diodes.

Introductory review articles on sub-Poissonian light have been given by Teich and Saleh (1990) and Rarity (1994). Undergraduate experiments to measure photon-counting statistics and to demonstrate sub-Poissonian light from an LED are described respectively by Koczyk *et al.* (1996) and Funk and Beck (1997).

Exercises

(5.1) A light beam of wavelength 633 nm and power 0.01 pW is detected with a photon-counting system of quantum efficiency 30% with a time interval of 10 ms. Calculate:

(a) the count rate;

(b) the average count value;

(c) the standard deviation in the count value.

(5.2) Calculate the probability of obtaining a count value in the range 48–52 in a Poisson distribution with an average value of 50. Compare the exact probability to that obtained by approximating the Poisson distribution to a Gaussian (normal) distribution and calculating the probability that the count value lies between 47.5 and 52.5. Try to repeat the exercise for a mean value of 100 and a range from 95 to 105.

(5.3) Prove eqn 5.30.

(5.4) Calculate the mean photon number per mode at 500 nm from a tungsten lamp source operating at 2000 K, and also the temperature required to achieve $\overline{n} = 1$ at this wavelength. What is the equivalent temperature for a wavelength of 10 μm?

(5.5) In an experiment to measure the photon statistics of thermal light, the radiation from a blackbody source is filtered with an interference filter of bandwidth 0.1 nm centered at 500 nm, and allowed to fall on a photon-counting detector. Calculate the number of modes incident on the detector, and hence discuss the type of statistics that would be expected.

(5.6) A pulsed diode laser operating at 800 nm emits 10^8 pulses per second. The average power measured on a slow response power meter is 1 mW. On the assumption that the laser light has Poissonian photon statistics, calculate the mean photon number and its standard deviation per pulse.

(5.7) The laser beam described in the previous question is attenuated by a factor 10^9. For the attenuated beam, calculate:

(a) the mean photon number per pulse;
(b) the fraction of the pulses containing one photon;
(c) the fraction of the pulses containing more than one photon.

(5.8) A beam with a photon flux of 1 000 photons s^{-1} is incident on a detector with a quantum efficiency of 20%. If the time interval of the counter is set to 10 s, calculate the average and standard deviation of the photocount number for the following scenarios:

(a) the light has Poissonian statistics;
(b) the light has super-Poissonian statistics with $\Delta n = 2 \times \Delta n_{\text{Poisson}}$;
(c) the light is in a photon number state.

(5.9) A 10 mW He:Ne laser beam at 632.8 nm is incident on a photodiode with a quantum efficiency of 90%. Calculate the noise power per unit bandwidth when the photocurrent generated by the laser flows through a 50 Ω resistor.

(5.10) Estimate the quantum efficiency of the detector used for the data shown in Fig. 5.11.

(5.11) The photodiode used for the data shown in Fig. 5.12 had a responsivity of 0.40 A W^{-1} at the laser wavelength. Estimate the power gain of the amplifier in dB units, on the assumption that the input impedance of the amplifier was 50 Ω.

(5.12) Consider the current flowing through a resistor R at temperature T in an ohmic circuit. The current fluctuations in a frequency band Δf are given by the Johnson noise formula:

$$\langle (\Delta i)^2 \rangle = 4k_{\text{B}}T\Delta f/R.$$

Show that the Johnson noise is smaller than the shot noise for the same average current value provided that the voltage dropped across the resistor is greater than $2k_{\text{B}}T/e$, and evaluate this voltage for $T = 300\,\text{K}$.

(5.13) The quantum efficiency of an LED is defined as the ratio of the number of photons emitted to the number of electrons flowing through the device. An LED emitting light at 800 nm is driven by a 9 V battery through a resistor with $R = 1000\ \Omega$. The LED has a quantum efficiency of 40%, and 80% of the photons emitted are focussed onto a photodiode detector with a quantum efficiency of 90%.

(a) Calculate the average drive current, given that the voltage drop across the LED is approximately equivalent to the photon energy in eV in normal operating conditions.
(b) Use the result in the previous exercise to calculate the Fano factor of the drive current for $T = 293\text{K}$.
(c) Calculate the average photocurrent in the detection circuit.
(d) Calculate the Fano factor of the photocurrent.
(e) Compare the photocurrent noise power in a 50 Ω load resistor with the shot-noise level for a bandwidth of 10 kHz.

(5.14) A laser pulse of energy 1 pJ and wavelength 800 nm is transmitted down an optical fibre with a loss of $3\,\text{dB km}^{-1}$. Calculate the maximum distance that the pulses can propagate before the probability that a pulse contains no photons exceeds 10^{-9}. Discuss the implications of this result for data communications.